The EMBO Journal Vol. 21 No. 22 pp. 6072–6082, 2002

Clathrin light and heavy chain interface: α-helix binding superhelix loops via critical tryptophans

Chih-Ying Chen, Michael L.Reese[1], Peter K.Hwang[2], Nobuyuki Ota[2], David Agard[2] and Frances M.Brodsky[3]

The G.W.Hooper Foundation, Department of Microbiology and Immunology and Departments of Biopharmaceutical Sciences and Pharmaceutical Chemistry, [1]Graduate Group in Biophysics and [2]Department of Biochemistry and Biophysics, University of California, San Francisco, CA 94143-0552, USA

[3]Corresponding author
e-mail: fmarbro@itsa.ucsf.edu

Clathrin light chain subunits (LCa and LCb) contribute to regulation of coated vesicle formation to sort proteins during receptor-mediated endocytosis and organelle biogenesis. LC binding to clathrin heavy chain (HC) was characterized by genetic and structural approaches. The core interactions were mapped to HC residues 1267–1522 (out of 1675) and LCb residues 90–157 (out of 228), using yeast two-hybrid assays. The C-termini of both subunits also displayed interactions extending beyond the core domains. Mutations to helix breakers within the LCb core disrupted HC association. Further suppressor mutagenesis uncovered compensatory mutations in HC (K1415E or K1326E) capable of rescuing the binding defects of LCb mutations W127R or W105R plus W138R, thereby pinpointing contacts between HC and LCb. Mutant HC K1415E also rescued loss of binding by LCa W130R, indicating that both LCs interact similarly with HC. Based on circular dichroism data, mapping and mutagenesis, LCa and LCb were represented as α-helices, aligned along the HC and, using molecular dynamics, a structural model of their interaction was generated with novel implications for LC control of clathrin assembly.

Keywords: cation–π interaction/clathrin/coat assembly/molecular dynamics/reverse two-hybrid screen

Introduction

Clathrin-coated vesicles (CCVs) mediate selective budding of receptors and ligands for endocytosis from the plasma membrane and for protein sorting from the *trans*-Golgi network during organelle biogenesis. On the cytosolic side of the membrane, the clathrin coat assembles into a polyhedral lattice that concentrates cargo proteins to specific sites within the membrane and contributes to membrane deformation for vesicle budding. Recent studies have identified regulatory proteins that influence cargo selection, membrane deformation, fission and uncoating (reviewed in Brodsky *et al*., 2001). However, clathrin itself has intrinsic properties regulating self-assembly that are not yet fully defined. In particular, critical self-regulation is imposed by the interaction of the clathrin light chain (LC) subunit with the heavy chain (HC) subunit. In this study, we characterize the structural features of the LC–HC interface to gain further insight into the process of CCV formation.

The assembly unit of the polyhedral clathrin lattice has a triskelion (three-legged) shape and is formed by three HC subunits, each with an associated LC subunit. The center of the triskelion, also known as the hub, comprises the C-terminal third of the HC (mammalian residues 1074–1675) and includes the region where three HCs trimerize (1550–1615) and radially extend into proximal leg domains (1074–1522) where LCs bind (Liu *et al*., 1995). Beyond the hub, the legs kink and the HCs fold into linear distal leg domains (Brodsky *et al*., 2001) adjacent to β-propeller N-terminal domains (TDs; residues 1–546) (ter Haar *et al*., 1998). TDs interact with adaptors and accessory factors involved in CCV formation. Clathrin HCs constitute the lattice backbone, and *in vitro* studies have demonstrated that LCs exert negative regulation over the spontaneous assembly of HCs (Ungewickell and Ungewickell, 1991; Liu *et al*., 1995; Ybe *et al*., 1998). In cells, this LC-dependent inhibition is overcome by participation of adaptor molecules in the assembly reaction. The heterotetrameric adaptor molecules induce clathrin lattice formation, link the lattice to membranes and sequester receptor cargo (Brodsky *et al*., 2001; Collins *et al*., 2002).

In vertebrates (mammals, fish and birds), there are two types of LCs with 60% sequence identity, LCa and LCb, encoded by different genes. In invertebrates (yeast, worms, *Aplysia* and *Drosophila*), there is only a single LC, but several LCs appear to exist in plants (Brodsky *et al*., 2001; Scheele and Holstein, 2002). The two vertebrate LC forms are expressed in all tissues at varying relative levels (Acton and Brodsky, 1990) and are distributed heterogeneously in clathrin triskelia (Kirchhausen *et al*., 1983). In neuronal cells, alternative splicing generates LCa and LCb isoforms, inserting 30 or 18 additional amino acids, respectively (Jackson *et al*., 1987; Kirchhausen *et al*., 1987). A linear arrangement of structural and/or functional domains in LCs has been defined and suggests multiple regulatory roles for LCs in CCV formation (reviewed in Brodsky *et al*., 1991). From the N- to C-termini, there is a conserved 22 residue sequence shared by all mammalian LCs with three negatively charged residues that regulate HC assembly (Ybe *et al*., 1998), a calcium-binding site, the HC-binding region, neuronal inserts and a calmodulin-binding site. There are also sequences unique to each of the LCs, including phosphorylation sites for casein kinase II on LCb and an hsc70-binding site in LCa.

LCs were shown to associate with the HC proximal leg domain by antibody localization (Kirchhausen *et al*., 1983; Ungewickell, 1983) and by *in vitro* binding assays (Näthke

et al., 1992; Liu *et al*., 1995). Genetic studies revealed that yeast LC binding depends on additional residues in the HC trimerization domain (Txd) (Pishvaee *et al*., 1997). In contrast, mammalian LCs will bind to HC fragments missing the Txd. Mammalian LCs bind the HC via their central region (Brodsky *et al*., 1987; Scarmato and Kirchhausen, 1990), which was previously predicted to participate in a coiled-coil interaction with the HC, based on sequence motifs detected in both subunits (Jackson *et al*., 1987; Kirchhausen *et al*., 1987; Näthke *et al*., 1992). However, the crystal structure of the LC-binding portion of the proximal leg domain of HC revealed that it is an elongated superhelix coil of short α-helices (Ybe *et al*., 1999). This finding, that the HC structure is not compatible with a classical coiled-coil interaction with the LC, prompted further analysis of the HC–LC interaction reported here.

Using yeast two-hybrid assays in combination with random PCR mutagenesis, we defined molecular contacts between the LC and the superhelical leg of the HC. This strategy selected first for mutants in LC that lost HC binding, and then for mutants in the HC partner that regained binding to the initial mutants. The first half of the scheme, also called a reverse two-hybrid assay, has been used often to analyze binding specificity (Vidal and Endoh, 1999). The other half takes advantage of the genetic concept of suppressors. This is, to our knowledge, the first example using these combined screens to dissect the molecular contacts of a protein–protein interface. Our results indicated that for LC to interact with HC, its central domain must maintain an α-helical structure. In addition, two contact sites between HC and LC were mapped at the molecular level, allowing us to generate a detailed structural model for subunit interaction. This model defines the extent of the HC–LC interface and suggests mechanisms for LC regulation of clathrin self-assembly.

Results

Defining minimal sites of HC and LC interaction

Boundaries of HC and LC interaction suggested by previous studies were defined by loss of activity upon proteolysis and deletion analysis (Scarmato and Kirchhausen, 1990; Näthke *et al*., 1992; Liu *et al*., 1995). We therefore undertook a 'positive' mapping of the minimal interacting domains. Fragments of bovine clathrin HC and LCb (neuronal form) were cloned into two-hybrid bait (pGBT9) and prey (pGAD424 or pACT2) vectors, respectively, to express the peptides fused to the GAL4 DNA-binding domain or the GAL4 activation domain. Consistent with previous findings (Liu *et al*., 1995), both the hub fragment (1073–1675) and the HC proximal leg (1073–1522) interacted effectively with full-length LCb when tested by two-hybrid assay (Figure 1A). Shorter HC fragments (1204–1522 and 1267–1522) apparently bound better to LCb than hub or the proximal domain, indicating possible inhibitory effects of HC regions beyond what is required for binding. Deletions at the N-terminus, after residue 1267, or at the C-terminus, before residue 1522, decreased HC fragment binding to LCb. When both ends were truncated simultaneously, the interaction of 1313–1481 with LCb was substantially weaker, suggesting that both ends of the 1267–1522

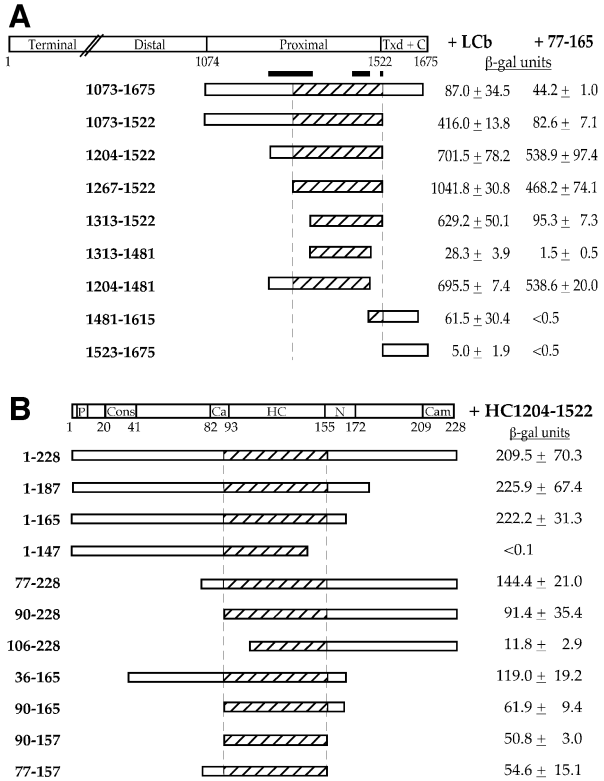

Fig. 1. Mapping minimal regions of clathrin HC and LC interaction. (**A**) Yeast SFY526 cells were co-transformed with the indicated bovine HC fragments (in pGBT9) plus full-length bovine brain LCb or the LCb fragment 77–165 (in pACT2). Quantitative β-galactosidase (β-gal) assays were performed, and results are shown in units as the mean ± SD of triplicate determinations. Above the fragments tested, a diagram of full-length HC is delineated, indicating the terminal, distal, proximal, trimerization and extreme C-terminal domains (Txd + C). Black bars below the HC diagram indicate sites previously implicated in LC binding (1213–1313, 1438–1481 and 1513–1522) (Näthke *et al*., 1992; Liu *et al*., 1995). Hatched lines within each fragment highlight the boundaries of the minimal region in HC (1267–1522) required for LC binding, mapped by these studies. (**B**) SFY526 cells were co-transformed with bovine HC fragment 1204–1522 (in pGBT9) and the indicated bovine brain LCb fragments (in pGAD424). Results of liquid β-gal assays are shown in units as the mean ± SD of triplicate determinations. Above the fragments tested, a diagram of full-length bovine brain LCb is delineated, indicating the phosphorylation domain (P), conserved region (Cons), calcium-binding site (Ca), previously predicted HC-binding site (HC), neuron-specific insert (N) and calmodulin-binding site (Cam). Hatched lines within each fragment highlight the boundaries of the minimal region in LCb (90–157) required for HC binding, mapped by these studies. The β-gal units shown in (A) are generally higher than those in (B) because LC fragments were constructed in different prey vectors in which pACT2 (for A) has a higher expression level than pGAD424 (for B).

minimal domain are involved in LCb binding. Nevertheless, the remaining weak interaction indicated that contacts with LCb must extend through the central portion of the HC minimal domain.

A shorter fragment of LCb (77–165), comprising the predicted central HC-binding region, bound most HC fragments but produced a weaker signal than full-length LCb (Figure 1A). No binding was detected to the most C-terminal HC fragments (1480–1615 and 1523–1675), which interacted weakly with full-length LCb, suggesting that the C-terminus of HC does not interact with the central region of LCb. Additionally, LCb 77–165 interaction with HC fragments was more sensitive to the presence of HC

residues 1267–1313 than full-length LCb, establishing an important contact site in that region. These data localize the minimal HC region required for efficient LC binding to between 1267 and 1522, overlapping most of the regions implicated in previous *in vitro* deletion studies (1213–1313, 1438–1481 and 1513–1522; Näthke *et al*., 1992; Liu *et al*., 1995), and define the N-terminal boundary more precisely to between 1267 and 1313.

The central region of LCb (90–157), comprising 10 heptad repeats and previously predicted to participate in a coiled-coil interaction (Jackson *et al*., 1987; Kirchhausen *et al*., 1987), bound HC fragment 1204–1522 (Figure 1B). Binding of LCb fragments truncated at the N-terminus after residue 90, or at the C-terminus before residue 157, was dramatically reduced or not detectable. LCb fragments extending just beyond the central region bound almost equally well to HC 1204–1522, establishing 90–157 as the minimal HC-binding region in LCb. However, full extension to the LCb N- and/or C-termini always resulted in better binding, suggesting that these additional sequences facilitate LC–HC interaction. Neither the calcium-binding site (82–93 in LCb) nor the neuronal insert (155–172 in LCb) was critical for HC binding.

Parallel interaction at the C-termini of HC and LC

It has been shown by electron microscopy that monoclonal antibodies recognizing the C-terminus of LCa decorate the C-terminal vertices of clathrin triskelia (Kirchhausen *et al*., 1983). Moreover, mutagenesis studies indicated that the C-terminus of yeast LC interacts with the Txd of the yeast HC (Pishvaee *et al*., 1997). To determine whether this is also the case for mammalian clathrin, a C-terminal HC fragment (1523–1675) comprising the vertex and the Txd was tested in combination with different LCb fragments. Only fragments containing the C-terminal portion of LCb (1–228, 77–228 and 154–228) were able to interact with the very C-terminus of HC (Figure 2). This correlates with the lack of binding by LCb 77–165 to C-terminal HC fragments shown in Figure 1A. Taken together, these results suggest that mammalian HC and LC contact in a parallel manner, at least at the C-termini, and that, similarly to yeast, the LCb-binding site in mammalian HC extends into the Txd.

Helical structure of the central region of LC is essential for HC interaction

To identify residues critical for interaction, *in vitro* random PCR mutagenesis (Muhlrad *et al*., 1992) was used to screen for mutations, in the central region of LCb, that abolished the interaction with HC fragment 1204–1522. Among ~2 × 10^4 colonies screened, 28 clones that failed to give positive interactions in the yeast two-hybrid assay were analyzed further. Most of the inserts from these clones either incorporated an early stop codon (Figure 3A) or generated out-of-frame/frameshift mutations (not shown). Ten clones, shown in Figure 3A, contained in-frame inserts with mutations in protein sequence. Interestingly, most of these non-binding mutant fragments incorporated helix breakers, such as proline or glycine, into their sequences. This supports the prediction that the central region of LCb is α-helical, and suggests that maintenance of this structure is crucial for HC binding.

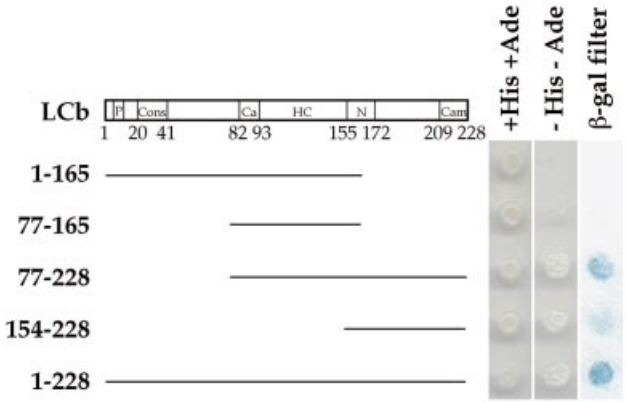

Fig. 2. Parallel interaction at the C-termini of clathrin heavy and light chains. Plate growth and β-galactosidase (β-gal) filter assays for the interactions between HC 1523–1675 and various LCb fragments. The boundaries of the LCb fragments tested are diagrammed relative to the full-length LCb sequence, with the functional domains delineated as defined in Figure 1B. For the plate growth assay, yeast AH109 cells were co-transformed with HC 1523–1675 (in pGBT9) and the indicated LCb fragments (in pACT2). The transformants were spotted onto plates lacking Leu and Trp, with (+) or without (–) His and Ade. Transformants expressing interacting constructs grew in the absence of His and Ade after 3–5 days. For the β-gal filter assay, SFY526 cells were co-transformed with HC 1523–1675 (in pGBT9) and the indicated LCb fragments (in pACT2). Transformants were spotted onto filters directly in contact with media and incubated for 2 days. Blue color indicating positive interaction developed within 6 h following substrate application in the filter assay. The assays shown are typical of three independent experiments.

To probe its helix-forming propensity, we monitored the circular dichroism (CD) of LCb in the presence of increasing concentrations of trifluoroethanol (TFE). TFE is a co-solvent commonly used to increase the helicity of peptides. LCb in an aqueous buffer exhibited a CD profile indicative of mixed helix/random coil conformation (Figure 3B), consistent with previous CD analyses (Ungewickell, 1983; Winkler and Stanley, 1983). The titration of LCb with TFE promoted conformational rearrangement that reduced random coil content and increased α-helical structure, evident in the spectral shifts at peak wavelengths 208 and 222 nm. This demonstrated that LCb has a tendency to form helices. Above 30% (v/v) TFE, the structure of LCb reached a maximal helical composition and was no longer sensitive to higher TFE concentrations.

To investigate whether HC binding affects LC structure, CD spectra of LCb were compared in the presence and absence of the HC proximal leg fragment (residues 1073–1522). The CD spectrum data for the proximal leg alone (Figure 3C) was consistent with the solved structure for residues 1210–1516, which fold into tightly packed α-helices (Ybe *et al*., 1999). The spectrum of a stoichiometric (molar ratio 1:1) mixture of LCb and the proximal leg exhibited stronger negative peaks at 222 and 208 nm than the calculated sum of the spectra of each protein alone. This clear difference between the model for non-interacting proteins (sum of spectra) and the experimental mixture indicates that secondary structure is induced upon interaction of LCb with HC. We attribute this change to LCb because crystallographic analysis and structural predictions suggest that the HC folds independently into

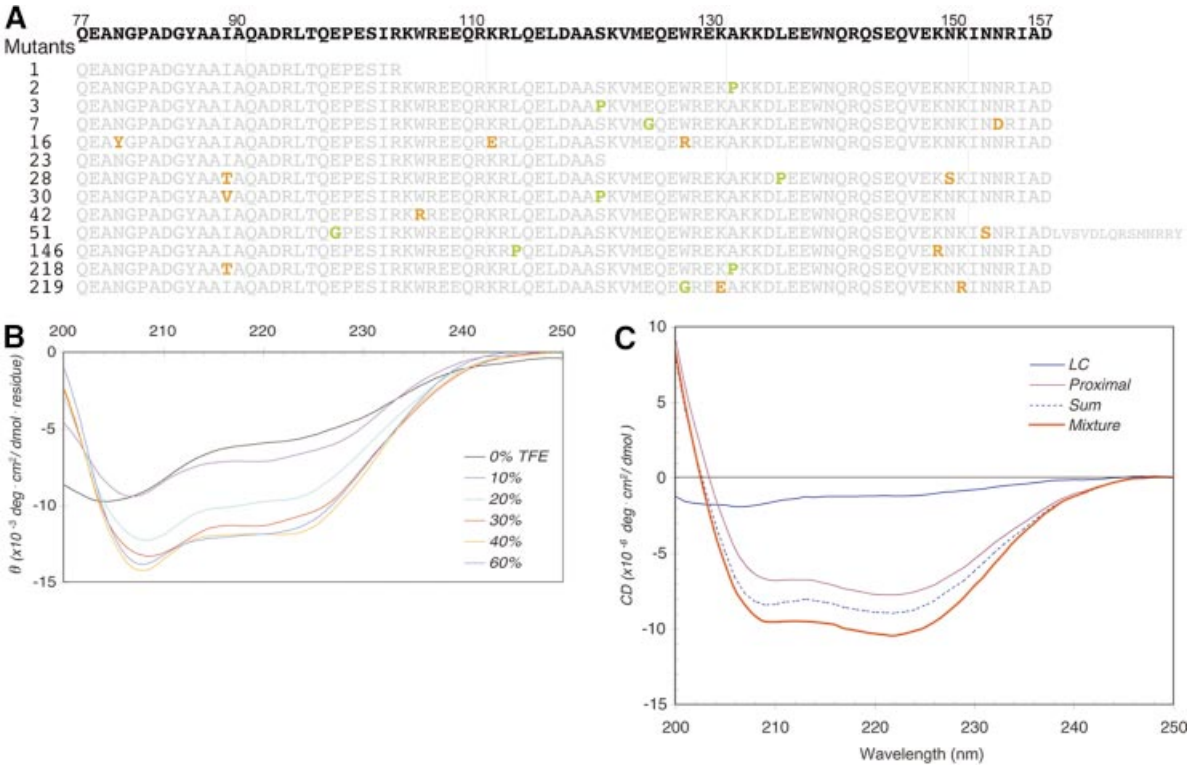

Fig. 3. Requirement for an α-helical conformation of clathrin LC during interaction with HC. (**A**) Sequences of the mutant fragments of bovine brain LCb 77–157 that were unable to bind HC. Yeast AH109 cells harboring HC 1204–1522 (in pGBT9) were co-transformed with mutated PCR products of LCb 77–157 and a gapped prey vector, pGAD424. The inserts of the recombinant clones (numbered mutants) unable to interact with HC 1204–1522 were sequenced. Mutated residues are in color and, among those, helix breakers are shown in green. (**B**) Far-UV CD spectra of LCb in the presence of TFE. Samples of LCb at a final concentration of 1.5 μM were incubated in 20 mM sodium phosphate buffer pH 7.1 with varying concentrations of TFE (0–60% v/v). CD intensity is represented as mean residue molar ellipticity. (**C**) Gain of signal for the LCb–proximal leg complex recorded by far-UV CD. The concentration of each indicated protein was 0.5 μM in 20 mM sodium phosphate buffer pH 7.1. The spectra of the isolated components, LCb, proximal leg and the complex are shown. The sum of the spectra of the two isolated proteins is also shown for comparison (dotted line). To facilitate the direct comparison of components with different numbers of residues, the CD intensity was calculated using the protein molar concentration rather than on a per residue basis.

a superhelix throughout the proximal and distal leg segments.

K1415 of HC interacts with LCb W127 and LCa W130

One isolated LC mutant (number 16) that was unable to bind HC did not include any helix breakers, but instead harbored three substitutions, N80Y, K111E and W127R (Figure 3A). Single mutations were constructed by site-directed mutagenesis to determine which of these mutations was responsible for loss of binding to HC. We found that the mutation at residue 127, from tryptophan to arginine, completely abolished the ability of full-length LCb to interact with wild-type HC fragment 1204–1522 (Figure 4A), while the other two mutations did not affect LC binding (data not shown). Apparently, LCb W127 plays a crucial role in contacting the HC.

To find the complementary binding site of LCb W127 on the HC, suppressor mutagenesis was performed. HC fragment 1204–1522 was subjected to error-prone PCR, and the product was co-transformed into yeast with the prey vector encoding LC mutant 16. The transformants that recovered binding to mutant 16 were selected and most of these contained a mutation of lysine to glutamate at 1415 (Figure 4B). Since LC mutant 16 used in the screen also included mutations other than W127R, single mutations subsequently were generated to confirm residues responsible for W127R binding. The single mutation of K1415E in HC fragment 1204–1522 rescued binding to full-length LCb W127R in a two-hybrid plate assay (Figure 4A).

To determine whether LCa shares HC-binding properties with LCb, the tryptophan residue corresponding to LCb W127 was mutated to arginine in LCa (W130R). Similar to its effect on LCb, this mutation in full-length LCa eradicated its binding to HC fragment 1204–1522, and mutation of HC K1415E recovered the binding (Figure 4A). The mutant HC fragment, however, still bound wild-type LCa and LCb, indicating that the mutation did not affect overall HC conformation or the conformation of the binding pocket for W127 or W130. To confirm the interaction at the protein level, an *in vitro* binding assay was performed. Purified His_6-tagged recombinant hub fragments (residues 1074–1675, wild-type or K1415E) first were immobilized on nickel affinity resin and incubated with lysates of bacteria expressing either wild-type LCb or the W127R mutant. Wild-type LCb bound efficiently to the hub fragment and the K1415E mutant hub (Figure 4C). In accord with the results described above, the LCb W127R fragment failed to bind hub, but did bind the K1415E mutant hub (Figure 4C). Furthermore, these protein assays established that LCb W127 is essential for LC binding even when additional C-terminal LC–HC

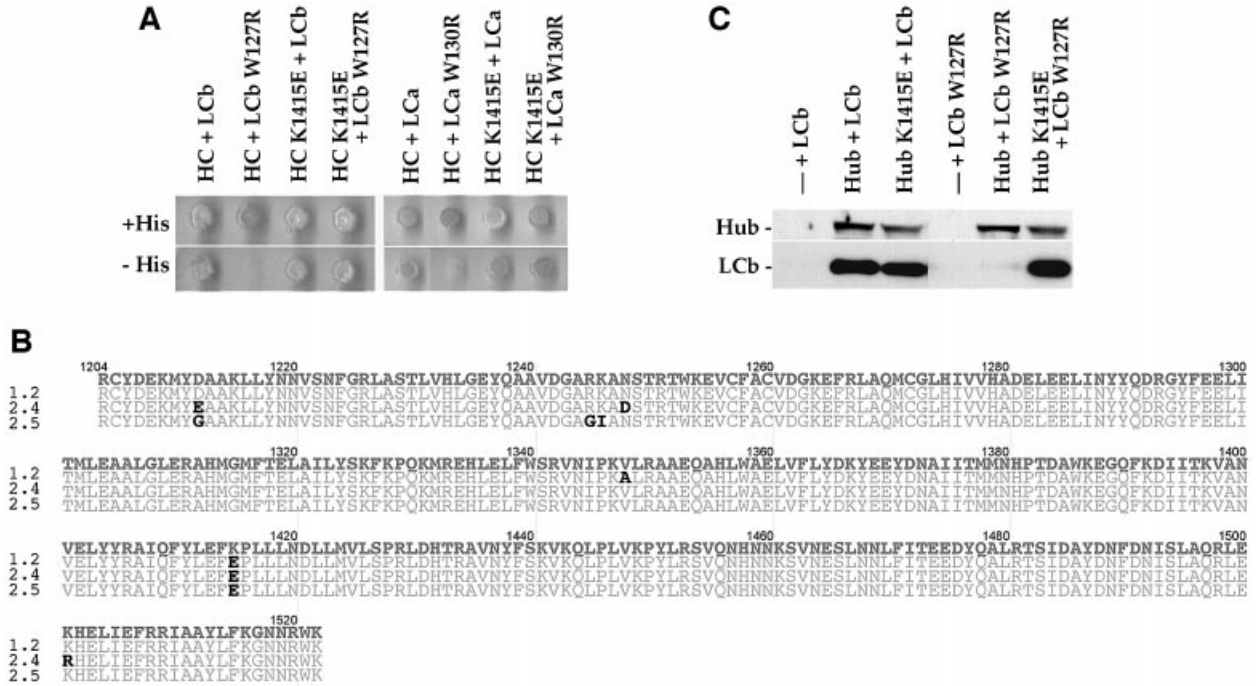

Fig. 4. Mutation of tryptophan to arginine at clathrin LC residue 127 in LCb or 130 in LCa abrogates binding to HC, which is rescued by HC mutation K1415E. (**A**) Plate growth assay of yeast AH109 cells co-transformed with HC fragment 1204–1522 (in pGBT9) and LCb/LCa (in pGAD424), with or without the indicated mutation. The transformants were spotted onto plates lacking Leu and Trp, with (+) or without (–) His. Transformants expressing interacting constructs grew in the absence of His after 2 days. (**B**) Sequences of bovine HC 1204–1522 mutants that rescued the binding to the LC mutant 16. AH109 cells harboring LCb mutant 16 (in pGAD424) were co-transformed with mutated PCR products of HC 1204–1522 and gapped bait vector, pGBT9. The transformants were selected for positive interactions. The inserts of the recombinant clones (1.2, 2.4 and 2.5) able to interact with the LC mutant 16 are shown. Mutated residues are in bold. The sequence of mutant 16 is in Figure 3A. (**C**) *In vitro* binding assays between recombinant hub fragments, with or without mutation K1415E, and wild-type or mutant LCb. Each purified hub fragment or no protein (–) was exposed to Ni^{2+} affinity resin and then incubated with lysates of bacteria expressing bovine brain LCb with or without the mutation W127R. Proteins bound to the affinity resin were eluted and analyzed for the presence of LC and hub fragments by immunoblotting with rabbit polyclonal antisera raised against the conserved region of LCs or the proximal region of HC, respectively.

contacts are present. The two-hybrid and binding data together demonstrated that HC K1415E can complement mutation of LCb W127R or LCa W130R and restore their loss of binding. However, mutation of this HC residue alone is not sufficient to abrogate LC binding by HC.

The K1326E mutation in HC rescues interaction with LCb W105R, W138R

Since the α-helical conformation of LC appears to be critical for HC interaction, we modeled the region of LCb 98–145 as an extended helix. When viewed from the C-terminus of this LC helix, two other tryptophan residues, W105 and W138, project from the same side as W127 (Figure 5A). The distance predicted between 105 and 127 is roughly twice that between 127 and 138. Given that LCb W127 is in contact with HC, we investigated whether these other two tryptophan residues also play a role in HC binding. LCb fragments with W105 and W138 residues mutagenized to arginine were generated for analysis by yeast two-hybrid assay. Single mutation of either W105R or W138R in LCb did not affect binding to HC fragment 1204–1522, yet LCb with both mutations W105R and W138R failed to interact with this HC fragment (Figure 5B, double mutant hereafter referred to as W105, 138R).

A suppressor mutagenesis screen was carried out to identify HC mutations (in fragment 1204–1522) that rescued binding to LCb W105, 138R. The K1326E mutation appeared in the sequences of almost all the rescuing clones (Figure 5C). By generating the single mutation of K1326E in the HC fragment, we confirmed that this mutation was sufficient to rescue binding to LCb W105, 138R (Figure 5B). Correspondingly, in a protein-binding assay, full-length LCb with the mutations of W105, 138R bound less efficiently to wild-type hub, but hub carrying the K1326E mutation recovered robust binding to the double mutant LCb (Figure 5D). As seen for the single K1415E mutation, the K1326E mutation in HC did not affect wild-type LCb binding. Unlike the non-binding LCb W127R mutant, some residual binding between LCb W105, 138R and hub was still detectable *in vitro*. This indicates that W105 and W138 are not as critical in LC–HC interaction as W127. Because mutation of neither W105 nor W138 alone was sufficient to abrogate HC binding, it is reasonable that a single mutation in HC restored the interaction with the double mutant in the two-hybrid assay. In fact, K1326E binding to LCb W105, 138R was sufficient to survive the challenge of 3-aminotriazole up to 60 mM (data not shown), a stringency test for this assay. Given the parallel orientation between the C-termini of HC and LC and the aligned interaction between HC K1415 and LCb

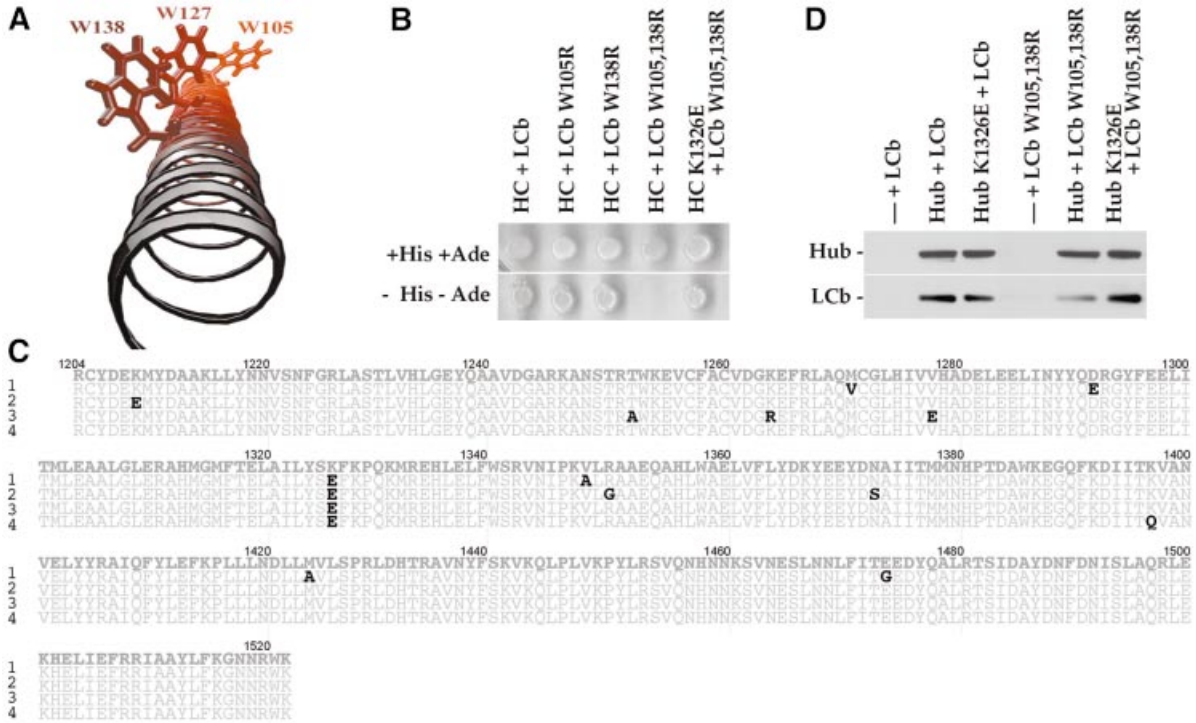

Fig. 5. Double mutation of tryptophan to arginine at clathrin light chain LCb residues 105 and 138 abrogates the binding to HC, and the interaction is rescued by HC mutation K1326E. (**A**) The three-dimensional structure of the central portion of LCb is modeled as an α-helix, viewed from the C-terminus. The predicted orientation of the side chains of tryptophan residues at positions 105, 127 and 138 is shown. (**B**) Plate growth assay of yeast AH109 cells co-transformed with HC 1204–1522 (in pGBT9) and LCb (in pGAD424), with or without the indicated mutation(s). The transformants were spotted onto plates lacking Leu and Trp, with (+) or without (–) His and Ade. Transformants expressing interacting constructs grew in the absence of His and Ade after 2 days. These results are representative of three independent experiments. (**C**) Sequences of bovine HC 1204–1522 mutants that rescued binding to the LC mutant W105, 138R. AH109 cells harboring the LCb W105, 138R mutant fragment (in pGAD424) were co-transformed with mutated PCR products of HC 1204–1522 and gapped bait vector, pGBT9. The transformants were selected for positive interactions. The inserts of the recombinant clones (1, 2, 3 and 4) able to interact with LCb W105, 138R mutant fragment are shown. Mutated residues are in bold. (**D**) *In vitro* binding assay (as described for Figure 4C) between recombinant hub fragments, with or without mutation K1326E, and wild-type or mutant LCb. LC and hub fragments were detected by immunoblotting with rabbit polyclonal antiserum raised against the conserved region of LCs or mouse monoclonal antibody against the His_6 tag epitope, respectively.

W127, we predict that HC K1326E is most probably rescuing interaction with LC W105R, and not with W138R.

Structural model of HC and LC interaction

The minimal HC-binding regions of LCa (93–160) and LCb (90–157) were modeled as α-helices and manually docked to the crystallographically determined structure of the HC proximal leg, fixing the mapped interaction pairs of HC K1415 with LCb W127 or LCa W130, and HC K1326 with LCb W105 or LCa 108, as constraints (Figure 6A). To create molecular models of the interfaces, a computer-generated simulation was performed for each LC–HC combination. A total of 150 copies of each protein fragment pair were equilibrated at 2000 K with the LC side chain atoms reduced in atomic radius, bond lengths, and electrostatic and van der Waals energies. The equilibrated molecules were then cooled slowly to 300 K, while growing the LC side chains to their original sizes and energies. During this annealing phase, the distances of the LC backbone carbonyls and amides were weakly restrained at 2.86 ± 0.5 Å in order to promote the helicity of the LCs. Additional restraints were applied between carbons of the aromatic rings of the LC tryptophan residues and their partner lysine amines. For each LC, a probability density map was constructed from the 150 model structures generated by this molecular dynamics approach, and a single model of the HC interface was best fit using crystallographic refinement techniques (Ota and Agard, 2001). In the resulting models, the HC-binding region of each LC was characterized as two contiguous α-helical segments that curve slightly along the length of the HC and bind via an essentially hydrophobic face. This is consistent with the prediction that the central region of the LCs forms an amphipathic helix. However, the models indicate that the primary LC-binding interface lies along the loop regions of the HC, rather than one of the helical faces, and the two subunits do not participate in a conventional coiled-coil interaction.

A closer look at the region predicted to surround LCb W127 (or LCa W130) showed the proximity of the LC tryptophan to HC K1415 (Figure 6B and D), consistent with the mutagenesis and binding data reported above. Notably, even when the constraint of LCb W127 or LCa W130 being near HC K1415 was dropped, the LC–HC docking models generated continued to place these residues in contact in the complexes. In these models, the LC tryptophan apparently stabilizes HC K1415 in an overall aromatic pocket of the HC core. The packing of the hydrocarbon arm of the lysine against the HC hydrophobic core was increased substantially from the unbound state,

and the amine was desolvated, allowing it to form strong cation–π interactions (Dougherty, 1996) with HC F1410 and the LC tryptophan.

Interestingly, while LCb W105 or LCa W108 were near HC K1326 in the models, they were too distant to be interacting directly. The predicted distance was ~8 Å while that between HC K1415 and LCb W127 (or LCa W130) was ~3 Å. In addition, the amine of K1326 was fully solvated, mitigating any interaction the charged group could have with an aromatic residue. Rather, LCb W105/LCa W108 appeared to be interacting with a pair of phenylalanine residues (F1296 and F1327), and LCb 101/LCa 104 were hydrogen-bonded with the backbone of the HC (Figure 6C and E). This is consistent with the mutagenesis data, which demonstrated a relatively weak interaction between W105 and the HC, but localized it to the area of K1326. It is important to note that the weak restraints used in the simulation were not sufficient to force an unfavorable interaction between the two residues in spite of their close proximity.

Discussion

Combining the screens of reverse two-hybrid and suppressor mutagenesis, we have established a novel approach to investigating the structural details of protein–protein interaction. This analysis has positively defined the essential regions for interaction of the clathrin HC and LC subunits, which were previously only inferred from negative deletion and proteolysis analysis. In addition, we have identified several molecular features critical for HC–LC binding. These data allowed the development of a three-dimensional model for the interface of HC and LC using molecular dynamics. The model suggests how the entire LC is oriented on the clathrin triskelion and has implications for LC control of clathrin assembly, discussed below.

Clathrin subunit interaction

Sequence analysis suggested that the central region of clathrin LCs forms amphipathic helices (Jackson *et al.*, 1987; Kirchhausen *et al.*, 1987). Earlier CD spectral analyses indicated a high α-helical content for purified clathrin (HC–LC complex) and a significantly lower content for isolated LCs (Ungewickell, 1983; Winkler and Stanley, 1983). The CD spectral analysis reported here demonstrates that free LC increases its helical structure in solvents favorable to helix formation or when mixed with its partner HC fragment. This is consistent with the mutagenesis data showing disruption of LC–HC binding by helix breakers. The emerging picture is that, during cellular biosynthesis of a clathrin triskelion, unstructured regions of LC fold in concert with docking to clathrin HC. This is similar to other well-characterized cases of protein folding induced by binding (Wright and Dyson, 1999).

The contact mapped between HC 1267–1522 and LCb 90–157 is fundamental for the core interaction of triskelion subunits. The structure of the proximal leg domain of HC is a superhelical rod of modular constituents [clathrin HC repeats (CHCRs)], each composed of 10 winding antiparallel α-helices (Ybe *et al.*, 1999). Based on the axial length of HC fragment 1210–1516 (115 Å), each residue spans an average 0.375 Å. Accordingly, the HC residues 1267–1516, involved in minimal LC binding, span ~100 Å, which accommodates LCb residues 90–157 (or LCa residues 93–160) modeled into an extended α-helix of 100 Å (Figure 6A). Thus the core LC–HC interaction covers ~60% of the proximal leg of the triskelion (Figure 7). Interestingly, the extended LC helix can be visualized as two contiguous helices of ~50 Å, each in contact with the loops of 10 HC helices, the length of a CHCR. Each LC helix segment is encoded by a separate exon (Stamm *et al.*, 1992), possibly reflecting complementary structural duplication in the two subunits.

Interactions independent of core binding were detected between the C-termini of HC and LCb, contributing positively to HC–LC binding affinity. This result is consistent with an earlier observation that the C-terminus of LC enhances its interaction with mammalian HC (Scarmato and Kirchhausen, 1990). In studies of yeast clathrin mutants, LC-binding regions in HC were demonstrated within the proximal leg and within the C-terminal Txd (Pishvaee *et al.*, 1997), and both sites were required for subunit interaction. We show here that mammalian LCb makes similar contacts, although it binds to the HC core in the absence of Txd sequences, suggesting stronger affinity between the mammalian subunits. Correspondingly, by two-hybrid analysis, we have observed that the whole extent of yeast hub (a trimer) is required for detectable yeast LC binding (C.-Y.Chen and F.M.Brodsky, unpublished data), while mammalian LCs bind shorter monomeric HC fragments (Figure 1). Specific binding between the vertex segment of HC and the C-terminus of LC reveals a parallel orientation of their interaction domains.

Molecular features of the HC–LC interface

A primary feature of our molecular models of LC–HC interaction is that the LC helix interacts with a surface comprised almost entirely of loops on the HC. The helix–turn–helix–loop structure of the HC proximal domain is a 24 × 28 Å oval in cross-section (Ybe *et al.*, 1999) (Figure 6A). This creates two major helical faces spanning

Fig. 6. Model of the contact between clathrin HC and LC. (**A**) A model of the interface of the minimal HC-binding region of LC (red) with the HC proximal leg (blue) produced by molecular dynamics calculations after alignment according to the mapping data produced in this study. The positions of the LC tryptophan residues involved in HC binding are indicated for the modeled segments of LCb 90–157 and LCa 93–160. Note that the HC modeling extends N-terminally to the major contact region, which begins at around residue 1267, and the extra helices project back from the interface. (**B**) The hydrophobic pocket of HC K1415 (purple) in contact with LCb W127. HC K1415 is sandwiched between the LC tryptophan and F1410, forming a strong cation–π interaction. (**C**) Interactions with HC in the region of LCb W105. While LCb W105 does not interact directly with HC K1326 (purple), it packs against the aromatic side chains of F1296 and F1327, which do interact. LCb S101 and LCa S104 are oriented to hydrogen-bond with the HC backbone. (**D**) The hydrophobic pocket of HC K1415 (purple) in contact with LCa W130, a cation–π interaction similar to that predicted for LCb W127. (**E**) Interactions with HC in the region of LCa W108. The interactions shown are similar to those predicted for LCb though the model indicates they are not as favorable. As our simulations were carried out with explicit hydrogens, their positions are included in the (B–E) and predicted hydrogen bonds are indicated by dashed lines. Figures were created using the Visual Molecular Dynamics program (Humphrey *et al.*, 1996) and rendered with Raster3D (Merritt and Bacon, 1997).

the length of the fragment and two thinner faces of loops between them. The LC contact points identified in this study, K1326 and K1415, are both located on one HC loop face (Figure 6A).

The region of the loop interface containing the K1415 pocket for W127 or W130 was well defined in both models of LC–HC interaction, as demonstrated by their low *B*-factors, values that indicate the degree to which their

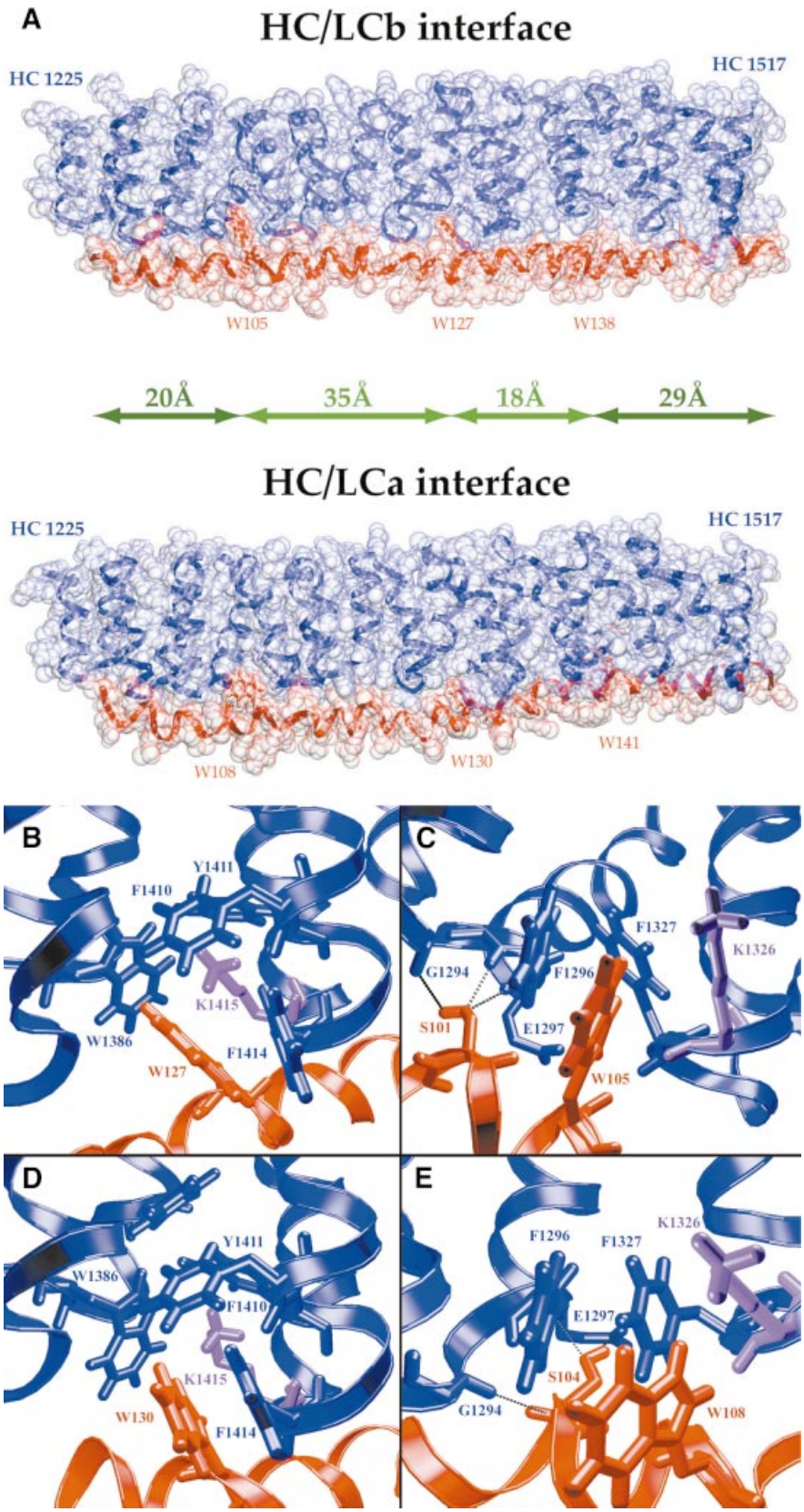

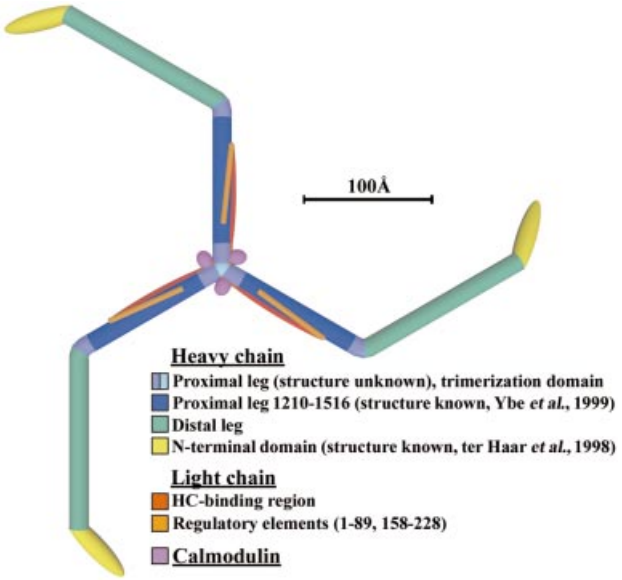

Fig. 7. Model of clathrin LC regulatory domains and their position on the clathrin triskelion. The HC-binding region (red) of the LC orients the Ca^{2+}-binding EF-hand towards the N-terminus of the proximal leg so that it may act as a structural switch to modulate the interaction of the N-terminal regulatory region (orange) of the LC with the HC. The predicted EF-hand is placed at the N-terminal red/orange junction. The C-terminus of the LC, with its calmodulin-binding site (also orange), is localized to the vertex of the triskelion. For neuronal CCVs where the calmodulin-binding site is exposed (Pley *et al*., 1995), calmodulin (purple) may modulate the preferred angle of the triskelion legs as they extend from the vertex. The model of the hub and distal leg segments was generated to scale based on electron microscopy measurements (Näthke *et al*., 1992), and the LC positioning is to scale based on the structural predictions discussed. TD and calmodulin are not drawn to scale.

positions are consistent in each individual structure determined (data not shown). The docking of LC W127/130 to HC K1415 was characterized by stabilizing cation–π interactions, common in protein interfaces (Gallivan and Dougherty, 1999). In addition, tryptophan is the most enriched residue in hot spots of protein–protein contact (Bogan and Thorn, 1998), suggesting a key role in binding specificity. Mutation of the central tryptophan, in the context of the full-length LC, completely abolished binding to hub (Figure 4), demonstrating that the cation–π interactions surrounding LC W127/130 provide both the specificity and a large portion of the binding energy that drive subunit interaction.

The proximity constraint for LCb W105 and HC K1326 generated models in this interface region which aligned neighboring LC residues with the HC loop face (e.g. LCb S101 forms three hydrogen bonds with the HC backbone at residues G1294, F1296 and E1297). The predicted hydrophobic pocket for HC binding to LCb W105 or LCa W108 was adjacent to but did not include K1326. Further modeling of the subunits with the mutations showed that HC K1326E rescued the binding of LCb W105R because the side chain of the arginine in LCb W105R could form a salt bridge with HC K1326E (data not shown). LCb W105 or LCa W108 apparently contributes less affinity to the HC–LC interface than the cation–π interaction of W127/130. LCb W105R reduced HC binding only when coupled to W138R, and LCa W108R reduced but did not eliminate HC binding (data not shown). The single mutation in LCa of W141R also reduced HC binding (data not shown). Thus, the third tryptophan (LCb W138 or LCa W141), that aligns with the other two (Figure 5A), is also located near or in the LC–HC interface. The slight displacement of this tryptophan relative to the HC interface is evident in both LC–HC models and emphasizes the curvature of the LC axis relative to the HC axis. This curvature might explain how distant mutations such as W105R and W138R could be synergistic in disrupting binding by altering the LC twist.

Though the models of the region around HC K1326 are apparently similar for LCb and LCa, binding of the LCa W108R mutant was not restored by the HC K1326E mutation (data not shown). This could be attributed to the subtle differences observable in the predicted disposition of each LC relative to the HC superhelix. Although such differences could be due to modeling limitations, they may actually reflect functional differences resulting from sequence divergence of LCa and LCb in their HC-binding regions.

Implications of the HC–LC interface for clathrin assembly

From analysis of the 21 Å resolution cryo-electron microscopy structure of a clathrin coat (Smith *et al*., 1998), it has been suggested that the proximal–proximal interactions between clathrin HCs involve the loops of the HC superhelix (Kirchhausen, 2000). However, our data clearly demonstrate that one of the loop 'edges' of the HC is occupied by the LC. It has been shown previously that LCs are readily dissociated from assembled clathrin baskets and are oriented on the lattice surface. Thus HC–HC interactions in the assembled lattice do not directly involve LCs, except for regulatory interactions. Consequently, we propose, based on our modeling, that the HCs most probably interact via their helical faces. This interaction would orient the LCs to the surface of the lattice, yet give them access to the interface to regulate assembly.

Our combined data and modeling establish the relative orientations of regulatory domains in mammalian LC with respect to the HC triskelion (Figure 7). This orientation suggests mechanisms of LC regulation of clathrin assembly in response to local intracellular calcium fluxes. Our model locates the predicted EF-hand of the LC Ca^{2+}-binding domain (Näthke *et al*., 1990) towards the N-terminus of the HC proximal leg. Structural EF-hands (e.g. those in calmodulin) experience large conformational changes upon Ca^{2+} binding. If this were also true for the LC EF-hand, it could act as a switch to control the N-terminus of LC folding back towards the C-terminus, along the segment of HC that is involved in the HC–HC interface. This bent LC conformation, predicted by antibody blocking studies (Näthke *et al*., 1992), potentially could inhibit proximal leg interaction with either the proximal or distal legs of neighboring triskelia by orienting residues in the N-terminal LC conserved region that have a negative regulatory effect on clathrin assembly (Ybe *et al*., 1998). All LCs contain the EF-hand motif, from mammalian to yeast, supporting the suggestion that the sensitivity of LCs to Ca^{2+} concentration is involved in their function.

Although the binding constant of LC for Ca^{2+} is relatively weak compared with that of calmodulin, it is conceivable that local intracellular Ca^{2+} concentrations could rise to a level that might influence clathrin assembly.

In order to transform from a planar lattice into a three-dimensional basket, the clathrin triskelia involved must undergo a change in pucker (Nossal, 2001), i.e. the relative angles of the legs to the plane of the trimerization domain must be altered. These angles may be controlled by Ca^{2+} concentration via calmodulin binding. Our data corroborate previous studies suggesting that the calmodulin-binding site of the LC C-terminus is near the triskelion vertex (Pley *et al*., 1995). With the binding of calmodulin, the triskelion vertex would become substantially more rigid, constraining the angle that triskelion legs could assume. Calmodulin appears to bind only the neuronal forms of LC in the context of a CCV (Pley *et al*., 1995), suggesting that such a mechanism could contribute to the uniformity of size observed for neuronal CCVs compared with CCVs in other cell types.

Our models place the Src family kinase HC phosphorylation site at Y1477 (Wilde *et al*., 1999) near the C-terminus of the minimal HC–LC interface. This proximity allows the possibility of additional regulation of clathrin self-interaction through phosphorylation of this site and subsequent modification of the HC–LC interface. An orchestration of these regulatory mechanisms for clathrin self-assembly probably contributes to controlling CCV formation.

Materials and methods

Yeast two-hybrid assays

HC fragments were amplified from bovine brain cDNAs (Liu *et al*., 1995) by PCR and cloned into the *Bam*HI–*Sal*I sites of pGBT9 (Clontech). LCb fragments were amplified from bovine brain cDNAs (Jackson *et al*., 1987) and cloned into either the *Eco*RI–*Bam*HI sites of pGAD424 (Clontech) or the *Bam*HI site of pACT2 (Clontech). Similarly, bovine LCa (Jackson *et al*., 1987) was amplified and cloned into the *Eco*RI site of pGAD424. Single residue mutations were generated with the quick-change site-directed mutagenesis kit (Stratagene). Yeast transformation (SFY526 or AH109), quantitative liquid β-galactosidase [using *o*-nitrophenyl β-D-galactopyranoside (ONPG) as substrate], filter and plate growth assays were performed following the Clontech yeast protocols handbook. For each indicated two-hybrid interaction, three different colonies were picked and each was assayed in duplicate.

PCR mutagenesis screens

Error-prone random PCR mutagenesis was carried out as described previously (Muhlrad *et al*., 1992). Briefly, target DNA was amplified using *Taq* polymerase (Promega) in a reaction mixture containing 3–6 mM $MgCl_2$, 0.1–0.6 mM $MnCl_2$, 1 mM dGTP, dCTP, dTTP and 0.2 mM dATP. The designed primers generated 85, 88 bp (or 90, 118 bp for suppressor screens) of homology flanking the gap of the vector for the recombination. In the reverse two-hybrid assay, the mutated PCR products of LCb 77–157 were transformed with gapped pGAD424 into AH109 cells carrying pGBT9 HC 1204–1522. Approximately 2×10^4 transformants appeared on SD –Leu –Trp plates after 3 days at 30°C and were then replica-plated onto SD –Leu –Trp –His –Ade plates. About 73 colonies that did not grow on the second plates were selected and tested again by streaking. The prey vectors from 28 confirmed colonies were isolated and the inserts were sequenced. Nine clones contained the exact length of the in-frame inserts with mutations, one with a longer insert (listed in Figure 3A), and the rest incorporated early stops or out-of-frame mutations. In the suppressor screens, the mutated PCR products of HC 1204–1522 and gapped pGBT9 were co-transformed into AH109 cells carrying either the prey mutant 16 or pGAD424 LCb W105, 138R. Transformants were selected on SD –Leu –Trp –His –Ade plates, and for each screen >90% of the rescued recombinant bait vectors shared the same mutation.

Circular dichroism spectroscopy

His_6-tagged proximal leg (1073–1522 in pET15b) was expressed in BL21 (DE3) cells and purified using Ni^{2+} affinity resin, followed by size exclusion chromatography, as described previously (Liu *et al*., 1995). Neuronal LCb co-expressed with the hub in pET15b (Liu *et al*., 1995) was partially purified by boiling and centrifugation (Näthke *et al*., 1992). CD spectra were obtained using a JASCO 715 spectropolarimeter equipped with a Peltier type cell holder for accurate temperature control. All measurements were conducted at 21°C in a 2 mm path length cell with protein concentrations of 0.5–1.5 μM in 20 mM sodium phosphate buffer, pH 7.1. Three to four averages were taken for each spectrum with the following parameters: step resolution, 0.2 nm; speed, 50 nm/min; response, 1 s; bandwidth, 1.0 nm. All spectra were corrected by subtraction of the corresponding spectra of blank samples.

Protein binding assay

Bovine hub fragment with an N-terminal His_6 tag (in pET15b) were expressed in bacteria and affinity purified using nickel resin, as described previously (Liu *et al*., 1995). Bovine brain LCb cDNA was cloned into the *Nco*I–*Bam*HI sites of pET15b (Novagen) to leave out the His_6 tag. LCb constructs were prepared in phosphate-buffered saline [pH 7.4, including 1 μg/μl protease inhibitors and 0.2 mM phenylmethylsulfonyl fluoride (PMSF)] as crude bacterial lysates. Protein concentration was determined by micro-BCA assay (Pierce). The LC-binding assay was modified from Liu *et al*. (1995). About 100 μg of purified recombinant hub fragment were bound to 100 μl of 50% Ni^{2+} affinity resin in 50 mM Tris–HCl pH 7.9 for 30 min. Lysates of bacteria expressing LCb (400 μg) were added to the bound resin and incubated for at least 30 min. After washing three times, bound proteins were eluted with 50 mM Tris–HCl pH 7.9, 0.5 M NaCl, 0.5 M imidazole. The bound fractions were subjected to SDS–PAGE and immunoblotted with a rabbit polyclonal antiserum against the conserved region of LCs (for LCb detection) (Acton and Brodsky, 1990) and a mouse monoclonal antibody to the His_6 tag (Clontech) or a rabbit polyclonal antiserum against the purified recombinant proximal leg of HC (produced by a contract laboratory for hub detection). Following incubation with horseradish peroxidase-conjugated goat anti-mouse/rabbit antiserum (ZyMed), the binding was detected by enhanced chemiluminescence (Amersham).

Modeling HC–LC interaction

Using the interaction pairs of LCb W105-HC K1326 and LCb W127-HC K1415 (or the corresponding W108, 130 in LCa) as guides, a helical model created in Quanta (Accelrys, Inc.) of LCb 90–157 or LCa 93–160 was docked manually to the HC proximal leg crystal structure (Ybe *et al*., 1999) by Molmol (Koradi *et al*., 1996). This docked model served as the starting point for the generation of an ensemble of 150 structures, which was refined to a single best-fit through multiconformational simulated annealing pseudo-crystallographic refinement (Ota and Agard, 2001). The final structure (Figure 6A) was refined against a pseudo-density map generated from the ensemble using standard crystallographic techniques.

Nuclear Overhauser effect (NOE) restraints were assigned between the Nζ and Cε of the HC lysine residues (K1326 and K1415) and each of the carbons of the aromatic ring of the partner tryptophan residues (W105/108 and W127/130, respectively). Structures were also calculated without the restraints in place to determine the degree to which the restraints forced the outcome (data not shown). These unrestrained structures were identical to the restrained structures calculated, within error. Additional NOE restraints were placed between the backbone carbonyls and amides of the LC in order to favor its helical structure. All calculations were carried out in X-PLOR (Brünger, 1992), using the OPLS force field for polar hydrogens (Jorgensen and Tirado-Rives, 1988) and the TIP3P model for water (Jorgensen *et al*., 1983).

Acknowledgements

We acknowledge Todd Graham for initiating the idea of the suppressor screens, and thank Ira Herskowitz and Linda Hicke for vectors, Diane Wakeham and Mhairi Towler for comments on the manuscript, Luke Rice and Zach Serber for helpful discussion, and Shu-Hui Liu and Christine Knuehl for technical advice. We acknowledge support from National Institutes of Health grants GM55143 and GM38093 to F.M.B. and training grant GM08284 to M.R., from the Arthritis Foundation for a postdoctoral fellowship to C.-Y.C., and from the Howard Hughes Medical Institute to N.O. and D.A.

References

Acton,S. and Brodsky,F.M. (1990) Predominance of clathrin light chain LCb correlates with the presence of a regulated secretory pathway. *J. Cell Biol.*, **111**, 1419–1426.

Bogan,A.A. and Thorn,K.S. (1998) Anatomy of hot spots in protein interfaces. *J. Mol. Biol.*, **280**, 1–9.

Brodsky,F.M., Galloway,C.J., Blank,G.S., Jackson,A.P., Seow,H.-F., Drickamer,K. and Parham,P. (1987) Localization of clathrin light-chain sequences mediating heavy-chain binding and coated vesicle diversity. *Nature*, **326**, 203–205.

Brodsky,F.M., Hill,B.L., Acton,S.L., Näthke,I., Wong,D.H., Ponnambalam,S. and Parham,P. (1991) Clathrin light chains: arrays of protein motifs that regulate coated vesicle dynamics. *Trends Biochem. Sci.*, **16**, 208–213.

Brodsky,F.M., Chen,C.-Y., Knuehl,C., Towler,M.C. and Wakeham,D.E. (2001) Biological basket weaving: formation and function of clathrin-coated vesicles. *Annu. Rev. Cell Dev. Biol.*, **17**, 517–568.

Brünger,A.T. (1992) *X-PLOR Version 3.1. A System for X-ray Crystallography and NMR*. Yale University, New Haven, CT.

Collins,B.M., McCoy,A.J., Kent,H.M., Evans,P.R. and Owen,D.J. (2002) Molecular architecture and functional model of the endocytic AP2 complex. *Cell*, **109**, 523–535.

Dougherty,D.A. (1996) Cation–π interactions in chemistry and biology: a new view of benzene, Phe, Tyr and Trp. *Science*, **271**, 163–168.

Gallivan,J.P. and Dougherty,D.A. (1999) Cation–π interactions in structural biology. *Proc. Natl Acad. Sci. USA*, **96**, 9459–9464.

Humphrey,W., Dalke,A. and Schulten,K. (1996) VMD: visual molecular dynamics. *J. Mol. Graph.*, **14**, 33–38.

Jackson,A.P., Seow,H.-F., Holmes,N., Drickamer,K. and Parham,P. (1987) Clathrin light chains contain brain-specific insertion sequences and a region of homology with intermediate filaments. *Nature*, **326**, 154–159.

Jorgensen,W.L. and Tirado-Rives,J. (1988) The OPLS potential functions for proteins. Energy minimizations for crystals of cyclic peptides and crambin. *J. Am. Chem. Soc.*, **110**, 1657–1666.

Jorgensen,W.L., Chandrasekhar,J., Madura,J.D. and Impey,R.W. (1983) Comparison of simple potential functions for simulating liquid water. *J. Chem. Phys.*, **79**, 926–935.

Kirchhausen,T. (2000) Clathrin. *Annu. Rev. Biochem.*, **69**, 699–727.

Kirchhausen,T., Harrison,S.C., Parham,P. and Brodsky,F.M. (1983) Location and distribution of the light chains in clathrin trimers. *Proc. Natl Acad. Sci. USA*, **80**, 2481–2485.

Kirchhausen,T. *et al*. (1987) Clathrin light chains LCa and LCb are similar, polymorphic and share repeated heptad motifs. *Science*, **236**, 320–324.

Koradi,R., Billeter,M. and Wuethrich,K. (1996) MOLMOL: a program for display and analysis of macromolecular structures. *J. Mol. Graph.*, **14**, 51–55.

Liu,S.-H., Wong,M.L., Craik,C.S. and Brodsky,F.M. (1995) Regulation of clathrin assembly and trimerization defined using recombinant triskelion hubs. *Cell*, **83**, 257–267.

Merritt,E.A. and Bacon,D.J. (1997) Raster3D: photorealistic molecular graphics. *Methods Enzymol.*, **277**, 505–524.

Muhlrad,D., Hunter,R. and Parker,R. (1992) A rapid method for localized mutagenesis of yeast genes. *Yeast*, **8**, 79–82.

Näthke,I., Hill,B.L., Parham,P. and Brodsky,F.M. (1990) The calcium binding site of clathrin light chains. *J. Biol. Chem.*, **265**, 18621–18627.

Näthke,I.S., Heuser,J., Lupas,A., Stock,J., Turck,C.W. and Brodsky,F.M. (1992) Folding and trimerization of clathrin subunits at the triskelion hub. *Cell*, **68**, 899–910.

Nossal,R. (2001) Energetics of clathrin basket assembly. *Traffic*, **2**, 138–147.

Ota,N. and Agard,D.A. (2001) Binding mode prediction for a flexible ligand in a flexible pocket using multi-conformation simulated annealing pseudo crystallographic refinement. *J. Mol. Biol.*, **314**, 607–617.

Pishvaee,B., Munn,A. and Payne,G.S. (1997) A novel structural model for regulation of clathrin function. *EMBO J.*, **16**, 2227–2239.

Pley,U.M., Hill,B.L., Alibert,C., Brodsky,F.M. and Parham,P. (1995) The interaction of calmodulin with clathrin-coated vesicles, triskelions and light chains. *J. Biol. Chem.*, **270**, 2395–2402.

Scarmato,P. and Kirchhausen,T. (1990) Analysis of clathrin light chain–heavy chain interactions using truncated mutants of rat liver light chain LCB3. *J. Biol. Chem.*, **265**, 3661–3668.

Scheele,U. and Holstein,S.E. (2002) Functional evidence for the identification of an *Arabidopsis* clathrin light chain polypeptide. *FEBS Lett.*, **514**, 355–360.

Smith,C.J., Grigorieff,N. and Pearse,B.M.F. (1998) Clathrin coats at 21 Å resolution: a cellular assembly designed to recycle multiple membrane receptors. *EMBO J.*, **17**, 4943–4953.

Stamm,S., Casper,D., Dinsmore,J., Kaufmann,C.A., Brosius,J. and Helfman,D.M. (1992) Clathrin light chain B: gene structure and neuron-specific splicing. *Nucleic Acids Res.*, **20**, 5097–5103.

ter Haar,E., Musacchio,A., Harrison,S.C. and Kirchhausen,T. (1998) Atomic structure of clathrin: a β propeller terminal domain joins an α zigzag linker. *Cell*, **95**, 563–573.

Ungewickell,E. (1983) Biochemical and immunological studies on clathrin light chains and their binding sites on clathrin triskelions. *EMBO J.*, **2**, 1401–1408.

Ungewickell,E. and Ungewickell,H. (1991) Bovine brain clathrin light chains impede heavy chain assembly *in vitro*. *J. Biol. Chem.*, **266**, 12710–12714.

Vidal,M. and Endoh,H. (1999) Prospects for drug screening using the reverse two-hybrid system. *Trends Biotechnol.*, **17**, 374–381.

Wilde,A., Beattie,E.C., Lem,L., Riethof,D.A., Liu,S.-H., Mobley,W.C., Soriano,P. and Brodsky,F.M. (1999) EGF receptor signaling stimulates SRC kinase phosphorylation of clathrin, influencing clathrin redistribution and EGF uptake. *Cell*, **96**, 677–687.

Winkler,F.K. and Stanley,K.K. (1983) Clathrin heavy chain, light chain interactions. *EMBO J.*, **2**, 1393–1400.

Wright,P.E. and Dyson,H.J. (1999) Intrinsically unstructured proteins: re-assessing the protein structure–function paradigm. *J. Mol. Biol.*, **293**, 321–331.

Ybe,J.A., Greene,B., Liu,S.-H., Pley,U., Parham,P. and Brodsky,F.M. (1998) Clathrin self-assembly is regulated by three light chain residues controlling the formation of critical salt bridges. *EMBO J.*, **17**, 1297–1303.

Ybe,J.A., Brodsky,F.M., Hofmann,K., Lin,K., Liu,S.-H., Chen,L., Earnest,T.N., Fletterick,R.J. and Hwang,P.K. (1999) Clathrin self-assembly is mediated by a tandemly repeated superhelix. *Nature*, **399**, 371–375.

Received August 12, 2002; revised and accepted September 19, 2002